Developmental Biology 396 (2014) 81–93

Contents lists available at ScienceDirect

Developmental Biology

journal homepage: www.elsevier.com/locate/developmentalbiology

A *Smad3* transgenic reporter reveals TGF-beta control of zebrafish spinal cord development

Alessandro Casari [a], Marco Schiavone [a], Nicola Facchinello [a], Andrea Vettori [a], Dirk Meyer [b], Natascia Tiso [a], Enrico Moro [c], Francesco Argenton [a,*]

[a] Department of Biology, University of Padova, I-35121 Padova, Italy
[b] University of Innsbruck, Austria
[c] Department of Molecular Medicine, University of Padova, I-35121 Padova, Italy

ARTICLE INFO

Article history:
Received 27 February 2014
Received in revised form
1 September 2014
Accepted 17 September 2014
Available online 5 October 2014

Keywords:
Smad3
Transcription
Reporter
TGFbeta
Transgenic
Zebrafish
Proliferation

ABSTRACT

TGF-beta (TGFβ) family mediated Smad signaling is involved in mesoderm and endoderm specifications, left–right asymmetry formation and neural tube development. The TGFβ1/2/3 and Activin/Nodal signal transduction cascades culminate with activation of SMAD2 and/or SMAD3 transcription factors and their overactivation are involved in different pathologies with an inflammatory and/or uncontrolled cell proliferation basis, such as cancer and fibrosis. We have developed a transgenic zebrafish reporter line responsive to Smad3 activity. Through chemical, genetic and molecular approaches we have seen that this transgenic line consistently reproduces *in vivo* Smad3-mediated TGFβ signaling. Reporter fluorescence is activated in phospho-Smad3 positive cells and is responsive to both Smad3 isoforms, Smad3a and 3b. Moreover, Alk4 and Alk5 inhibitors strongly repress the reporter activity. In the CNS, Smad3 reporter activity is particularly high in the *subpallium*, *tegumentum*, cerebellar plate, *medulla oblongata* and the retina proliferative zone. In the spinal cord, the reporter is activated at the ventricular zone, where neuronal progenitor cells are located. Colocalization methods show *in vivo* that TGFβ signaling is particularly active in *neuroD*+ precursors. Using neuronal transgenic lines, we observed that TGFβ chemical inhibition leads to a decrease of differentiating cells and an increase of proliferation. Similarly, *smad3a* and *3b* knock-down alter neural differentiation showing that both paralogues play a positive role in neural differentiation. EdU proliferation assay and pH3 staining confirmed that Smad3 is mainly active in post-mitotic, non-proliferating cells. In summary, we demonstrate that the Smad3 reporter line allows us to follow *in vivo* Smad3 transcriptional activity and that Smad3, by controlling neural differentiation, promotes the progenitor to precursor switch allowing neural progenitors to exit cell cycle and differentiate.

Introduction

TGFβ1/2/3, Activin/Nodal and BMP signaling belong to the TGFβ family. All three signaling subfamilies show a similar transduction pathway: the secreted ligands interact with type I and II transmembrane serine-threonine kinase receptors. The type II receptors phosphorylate type I receptor, which in turn permits the binding of receptor-regulated transcription factors SMADs (R-SMADs) and their subsequent phosphorylation at the C-terminus. Activated R-SMADs can interact directly with a common mediator, SMAD or Co-SMAD (SMAD4), and then translocate into the nucleus to directly target gene expression (Moustakas and Heldin, 2009).

BMP, Activin/Nodal and TGFβ1/2/3 signaling require different ligands, type II receptors (ALK1, 2, 3 and 6 for BMP; ALK4, 5 and 7 for TGFβ1/2/3 and Activin/Nodal) and R-SMADs (SMAD1, 5 and 8 for BMP; SMAD2 and 3 for TGFβ1/2/3 and Activin/Nodal) (Hinck, 2012). As a consequence, gene sequences recognized by R-Smads are different for the two signaling pathways. In zebrafish two *smad3* isoforms are known: *smad3a* and *3b*. They are the result of the genome duplication that occurred during teleost evolution. These two genes show a partially overlapping expression: they are both expressed in the tail bud and lateral stripes of the forming mesoderm; however, Smad3a is also produced in an additional area that surrounds the tail bud (Dick et al., 2000). Their mechanisms are similar and they are expressed in overlapping and non-overlapping tissues (Pogoda and Meyer, 2002) displaying additive genetic effects.

* Corresponding author.
E-mail address: francesco.argenton@unipd.it (F. Argenton).

http://dx.doi.org/10.1016/j.ydbio.2014.09.025

All the TGFβ1/2/3 and Activin/Nodal *R-smads* and *smad4* transcripts are ubiquitously expressed since blastula stage as a consequence of their maternal origin (Dick et al., 2000). However, during gastrulation, they are either transcribed at very low level (*smad2*), or almost undetectable (*smad3a* and *3b*) (Dick et al., 2000; Pogoda and Meyer, 2002). In contrast, *smad4* expression is high in all these stages (Dick et al., 2000). From tail bud stage *smad3a* and *3b* mRNA production increases (Hsu et al., 2011). At late somitogenesis (16 hpf) *smad3a* mRNA is mainly confined to the eyes and tail region, although present at low levels throughout the embryo. *smad3b* is expressed in the same areas, but it has a higher rate of expression overall (Hsu et al., 2011). Both *smad2* and *4* are present in the entire embryo, but particularly in the tail region, the eye and the brain (Hsu et al., 2011). However, *smad2* and *3* expression is necessary but not sufficient for correct functionality: a signal transduction cascade leading to their phosphorylation is needed (Liu et al., 1997).

Although Smad2 and 3 share a highly similar protein structure (more than 90% amino acid sequence identity), they are involved in different physiological and pathological processes. Smad2 knockout mice fail to form mesoderm and endoderm demonstrating the importance of this transcription factor in early development (Nomura and Li, 1998). Smad3 knockout mice, while viable, have chronic intestinal inflammation producing colorectal cancer and metastasis (Zhu et al., 1998). Therefore, Smad3 transcription factor seems to be associated to the immune system and it might regulate cell cycle working as tumor suppressor. These different roles correlate with their slightly different structure. Smad2 contains an inhibitory region in the MH1 region that hinders direct DNA binding. In contrast, Smad3 recognize Smad Binding Element (SBE) boxes that were used for the creation of the Smad3-responsive line of this work. Furthermore, a Smad2 alternative splicing variant missing the inhibitory domain has been reported. This variant would bind DNA directly and is possibly responsible for Smad2's impact during development (Dunn et al., 2005; Lee et al., 2011).

R-SMADs activity is regulated by inhibitory-SMADs (I-SM ADs). For TGFβ, SMAD7 functions as a negative signaling regulator (ten Dijke and Hill, 2004). The inhibitory factor SMAD7 is induced by SMAD3 and provides a negative feedback loop to the pathway. In zebrafish, *smad7* shows a pattern of expression similar to that observed for *smad3b*, underlying the reciprocal functional connection between the two genes. *smad7* is ubiquitously present as maternal transcripts until gastrula stage, when its expression decreases, becoming limited to the ventral side of the embryo, though expression increases in the tail bud (Pogoda and Meyer, 2002). SMAD7 can act in different ways: it can compete with R-SMADs for binding type I receptors; it can recruit E3-ubiquitine ligases (SMURF1 and 2) to the activated type I receptors causing their degradation (ten Dijke and Hill, 2004).

TGFβ signaling is involved in a wide range of physiological and pathological processes in both embryonic and adult stages. It acts as a morphogen through Nodals and Activins directing the patterning of the three germ layers (Watabe and Miyazono, 2009). A dysregulation of this pathway is associated with tumorigenesis, fibrosis, allergic response and neurodegenerative diseases. Both in physiological and pathological conditions, its effect depends on the tight regulation of the cell cycle (Fleisch et al., 2006). TGFβ signaling is a well-known pro-apoptotic signal, it promotes epithelial-to-mesenchymal transition (EMT) (Song, 2007) and SMAD4 is a powerful tumor suppressor in pancreatic tumors (Herman et al., 2013). In the etiopathogenesis of neurological disorders the role of SMAD3/TGFβ signal is not so clear; TGFβ signaling disruption is correlated with several motor neuronal diseases, because of the neuroprotective and anti-inflammatory effects of this pathway (Katsuno et al., 2011). Its overactivation is associated with the formation of β-amyloid plaques in Alzheimer's disease (Town et al., 2008). TGFβ seems to be involved in glial differentiation and production of extracellular matrix (ECM) components for the scaffolding of neurons in the neural tube. Moreover, it is also a neurotropic factor that stimulates neurogenesis and axon growth (Gomes et al., 2005).

Dennler et al. have found specific binding sequences for SMAD3 in the hPAI gene promoter (Dennler et al., 1998). These sequences (so-called CAGA box) are specifically recognized by the SMAD3/SMAD4 complex. Due to an intrinsic steric hindering, SMAD2 cannot interact directly with CAGA box (Dennler et al., 1998). Taking advantage of this specificity, we have developed transgenic reporter lines containing multimerized "CAGA box" to study *in vivo* Smad3-mediated signaling. Genetic, pharmacological and molecular analyses show that in these transgenic lines the reporter gene is activated in a Smad3/TGFβ-responsive manner. During embryo development, reporter expression was mainly found in the central nervous system (CNS). In order to determine the role of TGFβ in neural development, we have performed a series of experiments using the Smad3-responsive line crossed with transgenic fish lines reporting different stages of the progenitor to precursor development. To take advantage of all potentialities of transgenic lines in reporting fluorescent signal dynamics, the majority of analyses have been performed *in vivo*. Results show that postmitotic activation of TGFβ in neural cells controls the progenitor to precursor transition. Finally, we predict that this line might be a valuable tool in drug screening as well as in regeneration and cancer research.

Materials and methods

Animals

Animals were staged and fed as described by Kimmel et al. (1995). The project was examined and approved by the Ethics Committee of the University of Padua with protocol number 18746. *one-eyed pinhead* (*oep*^{m134}) (Schier et al., 1996) and *chordin* (*din*^{tt250}) (Schulte-Merker et al., 1997) mutant carriers were identified both by PCR analysis and phenotype screening of their offspring at 24 hpf. For *oep* PCR screening, the following primers were used: oepm134-wtFw (5′-GGCTCC CTCAGAACACTGTC-3′), oepm134-mutRv (5′-GGCTCCCTCAGAACACT GTA-3′) and oepm134-Rv (5′-CTCTTGGGCACAAAAGAGAA-3′). For *dino* PCR screening, the following oligonucleotides were used: dino-Fw (5′-GACACAAATGCGGGGTAAAC-3′), dino-Rv (5′-ATGTTGCAACTCAG-CAGCAG-3′), dino-wtRv (5′-CTGTGCACAACTCAC-3′) and dino-mutRv (5′-ACTGTGCACAACTCAC-3′). For functional *in vivo* studies we used the following transgenic lines: Tg(*ngn1:GFP*)sb1, Tg(*mnx1:GFP*)ml2. For *neuroD*, we used the Tg(*−2.4 kb neurod:EGFP*) line previously produced in our lab (see also Ronneberger et al., 2012): briefly, the 2.4 kb promoter of zebrafish NeuroD coding gene was cloned in the pG1 vector and the resulting linearized plasmid injected in fertilized eggs. The F1 progeny was screened for GFP expression in the CNS. For *smad7* overexpression, we used the Tg(*hsp70:smad7-YFP*) line (not published, see below). For all the described experiments, heterozygous embryos and larvae were used.

Generation of Tg(12xSBE:EGFP)ia16 and Tg(12xSBE:nls-mCherry)ia15 lines

12 repeats of a Smad3-binding sequence, so called CAGA box (Dennler et al., 1998), were amplified together with major late promoter Adenovirus (MLP) with the attB4cagafor (5′-GGGGA-CAACTTTGTATAGAAAAGTTGGCCCGGGCTCGAGAGCCAG-3′) and attB1-cagarev (5′-GGGGACTGCTTTTTTGTACAAACTTGTTGGAAGAGAGTGAGG ACGAA-3′) oligonucleotides and then cloned into a pDONOR™ P4-P1R

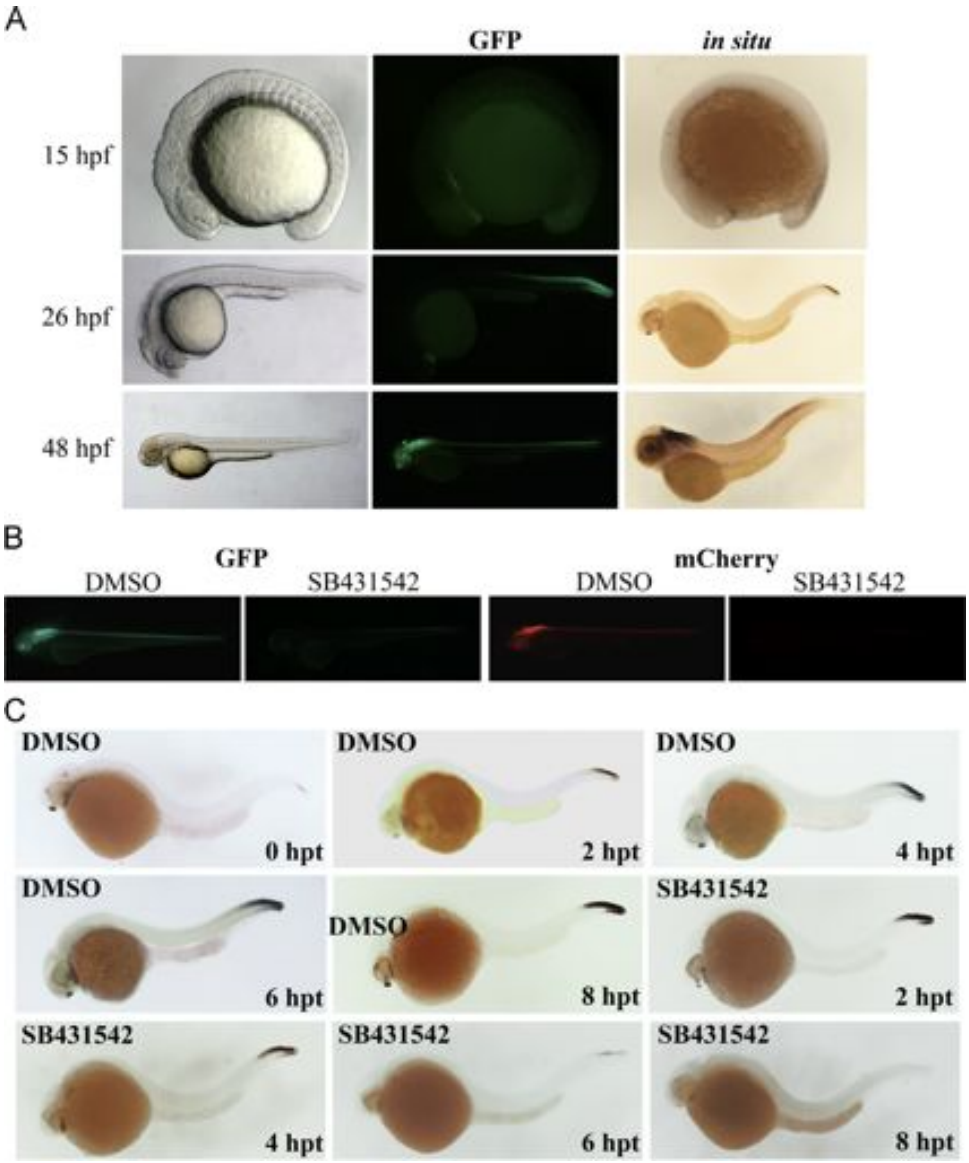

Fig. 1. D12xSBE lines are reporters of TGFβ signaling. (A) Brightfield, fluorescence and *in situ* hybridization lateral views of Tg(*12xSBE:EGFP*)ia16 embryos at 15, 26 and 48 hpf, anterior to the left. GFP expression appears in late somitogenesis in the tail and cardiac mesoderm region. At 26 hpf GFP is visible in the telencephalic region and expressed in the embryo neural tube and tail. At 48 hpf reporter expression is extended to the entire neural tube, maintaining a decreasing gradient from the tail, and in some areas of the brain. Transcription (*in situ*) and translation (GFP) patterns are coherent. (B) Fluorescent images of 3 dpf larvae of Tg(*12xSBE:EGFP*)ia16 (in green) and Tg(*12xSBE:nlsmCherry*)ia15, (in red) either treated with the Alk4- and Alk5-inhibitor SB431542 or with carrier (DMSO) for two days: lateral views, anterior to the left. **C**. RNA *in situ* hybridization for EGFP mRNA performed in embryos of Tg(*12xSBE:EGFP*)ia16 treated at 24 hpf with the Alk4- and Alk5-inhibitor, SB-431542 and fixed at different time points: 2, 4, 6, 8 h post treatment (hpt).

according to the manufacturer's guidelines (Invitrogen Multisite Gateway System, CA). The resulting Gateway 5′ entry vector was recombined with a middle entry vector containing a reporter gene (*EGFP, nls-mCherry*), pME vector (pME-EGFP, pME-nlsmCherry), and a 3′ entry vector containing *SV40-polyA* sequence (p3E-polyA) (Kwan et al., 2007). 25–50 pg of the obtained Tol2 vector containing Smad3-responsive sequences was co-injected together with 25 pg of *in vitro* synthesized Tol2 Transposase mRNA into one-cell stage wild-type embryos. Mosaic transgenic fish were selected at approximately 24 h post-fertilization (hpf) for fluorescent expression and raised to the adult stage for screening. Positive founders were selected for the fluorescence level of their offspring in areas of known Smad3 activity and by checking responsiveness of reporter expression to SB-431542 (S4317, Sigma, MO), a known Alk4- Alk5-inhibitor (Fig. 1). One allele for each EGFP and nls-mCherry reporter line was selected and used to follow *in vivo* Smad3-mediated TGFβ signaling.

Chemical treatment and RNA in situ hybridization

SB431542 (S4317, Sigma, MO), LY364947 (L6293, Sigma, MO) and LDN193189 (SML0559, Sigma, MO) were solubilised in pure DMSO to 100 mM, 6 mM and 10 mM final concentrations, respectively. For treatment at 24 hpf, SB431542, LY364947 and LDN193189 were diluted in zebrafish fish water containing 2 mM 1-phenyl-2-thiourea (PTU) to have working solutions of 100 μM, 40 μM and 10 μM, respectively. For LY364947 treatment at 2 hpf, we used a final concentration of 10 μM in zebrafish fish water. Treatments were carried out in 6 or 24 well-plates. When needed, embryos and larvae were fixed in 4% paraformaldehyde (PFA)/PBS overnight at 4 °C and then stored in pure methanol at −20 °C. Whole mount RNA *in situ* hybridizations were performed as described before (Thisse et al., 1993). EGFP probe was produced using DIG-labeled ribonucleotides, T7 RNA polymerase and linearized pME:EGFP supplied by Tol2 kit.

Morpholinos injections

smad2, *3a* and *3b* knock-down were carried out injecting morpholinos previously tested by Jia et al. (2008): MO-*smad2* 5′-TTACCCTTCCTACGAAAAGCGTTCT-3′, MO-*smad3a* 5′-TTCAGTTCAGCGTTCCTTCCTCTATTGC-3′ and MO-*smad3b* 5′-TTGTCCACGAGTCACATCACCGCAT-3′. For coinjection of smad2 and smad3a morpholinos, lower doses of each one were injected in 1–2 cell stage embryos of Tg(*12xSBE:EGFP*)ia16.

For the study of putative co-interaction between *smad2* and *3a* morpholinos, the lowest doses associated with the minimal percentage of malformed embryos (lowest effective doses) were used to prepare the morpholinos mix.

For *smad4*, GeneTools, LLC, OR synthesized four different morpholinos targeting this gene at either the start-codon or one of three different splicing sites: MO4(1) 5′-TCTCGCCCACCTGAACGTCCATCTC-3′, MO4(2) 5′-TACTGATGTTGACGCTCTACCTCGC-3′, MO4(3) 5′-GCAGTCTGAAAACAGAGAAGTCAGA-3′ and MO4(4) 5′-GTGTATGTGTTTCTCACCTTGATGT-3′. All of them were injected in drops of 500 pL at 1 mM concentration in Tg(*12xSBE:EGFP*)ia16 eggs. Effects on embryo morphology and EGFP expression were observed at 24 hpf. MO4(3) was used for *in vivo* experiments at lower concentration (0.5 mM). To verify its ability to control BMP signaling, it was also tested in the Tg(*BMPRE:EGFP*)ia18 line. As a control, we injected the generic control morpholino supplied by GeneTools (MO-CTL).

smad2 and *4* morpholinos target a splicing site. Therefore, they have been further validated through RT-PCR. For *smad2*, the following primers have been used: Fw 5′-GGCTACAGTGGGAAGGAAAA-3′ and Rv 5′-GGTATCCCACTGTTCTATCGTATTT-3′. For smad4, the following primers have been used: Fw 5′-GCGTCCAGCTGGAGTGTAAA-3′ and Rv: 5′-CGATCCAGCAGGGCGTCTCTTT-3′.

smad3a and *3b* morpholinos target the start codon. Therefore, they have been further validated through whole-mount immunohistochemistry for phospho-Smad3 (ab52903, Abcam, Cambridge, UK).

smad2, 3a, 3b and 4 mRNAs injections

smads coding cDNA are contained in pCS2+ plasmids. Each plasmid was digested with a specific restriction enzyme (EcoRI/XhoI for *smad2*, *3b* and *4* plasmids; BamHI/EcoRI for *smad3a* plasmid) and then used for gene transcription through SP6 RNA polymerase (AM2071, Lifetechnology, CA). Four different dilutions (100, 50, 20 and 1 ng/μl) of each mRNA was injected in drops of 500 pL in 1–2 cell stage embryos of Tg(*12xSBE:EGFP*)ia16 line. Their effect on GFP expression was evaluated at 24 hpf at the epifluorescent microscope.

Heat-shock induced overexpression of smad3b and smad7

Cloning of *hsp70:Smad7-hsp70:YFP* and *hsp70:smad3b-hsp70:YFP* constructs: pCS2+ containing full- length *smad7* cDNA or PCR-modified coding region of *smad3b* were linearized and cut to insert an *hsp70:YFP* cassette. In a second step *smad3* or *smad7-hsp70:YFP* was cut out and cloned into the EcoRV/Acc651 sites of the hsp70 containing vector p2hsp70 (gift from Nico Scheer and Jose Campos-Ortega). The *hsp70:smad7-hsp70:YFP* containing vector was injected in 1–2 cell stage embryos to obtain a stable transgenic line: Tg(*smad7-hsp70:YFP*).

To validate the Tg(*12xSBE:nls-mCherry*)ia15 line, we stimulated overexpression of *smad3b* and *smad7*: we injected 1–2 cell stage embryos of 12xSBE line with a plasmid containing the *smad3b* sequence in frame with *YFP* sequence under the control of heat-shock 70 promoter (*hsp70*). For *smad7*, the Tg(*12xSBE:nls-mCherry*)ia15 line has been crossed with the Tg(*hsp70:smad7-YFP*) line. In both cases, heat-shock was performed 3 times for 30′ at 37 °C every 12 hours starting from 24 hpf. Larvae were observed at the confocal microscope 2 h after the third heat-shock.

Confocal analysis and colocalization measurements

Fluorescence was visualized at the Leica M165FC dissecting microscope and then at the Nikon C2 H600L confocal microscope. For *in vivo* analyses embryos and larvae were anesthetised with tricaine and mounted in 0.7% low melting agarose gel. EGFP and mCherry fluorescence was visualized by using 488 and 561 nm lasers, respectively, through 20x and 40x immersion objectives (Nikon). All images were analyzed with Nikon software. Colocalization was measured with Volocity 6.0 software. Statistical analyses were carried out with Prism GraphPad software. For analysis of Smad3/TGFβ signal dynamics at 24 hpf, we mated Tg(*12xSBE:nls-mCherry*)ia15 with the following transgenics: Tg(*ngn1:GFP*)sb1, Tg(*−2.4 kb neurod:EGFP*), Tg(*mnx1:GFP*)ml2. Between 15 and 24 hpf somites are formed at a rate of 2/h; thus, each somite corresponds to a point in time expressed in hours of development. Colocalization was expressed as Manders' coefficient (Manders et al., 1993; Dunn et al., 2011) and refers to mCherry/TGFβ. It was measured in 4 sequential somites pairs (tail to head), and 6 tails were analyzed. Resulting values were plotted as a function of somite/time (as hours of development). Manders' coefficients M1 and M2 are defined as the proportion of intensity in Red channel (TGFβ reporter) that coincide with intensity in the Green (progenitor/precursor) channel (Manders et al., 1993). Mander's coefficients were used in place of Pearsons' because M1 and M2 are less dependent on the intensity ratios between channels and the intensity is considered as amount of fluorescence, not as volume occupied by each channel. Therefore, if one channel occupies a larger volume than the other (as registered with TGFβ/mCherry and the three neural markers/GFP), Manders' coefficients can better measure any correlation between them. For each type of experiment, a number of embryos or larvae (from 15 to in excess of 100) were sampled and the correlation between treatment and phenotype quantified. Results of quantification are presented in Supplemental Table S1. For all the experiments of quantification, we used heterozygous embryos and larvae derived from oucrossing a transgenic male of the ia15 or ia16 lines.

Whole-mount immunohistochemistry

Embryos and larvae were fixed in 4% PFA/PBS overnight and then stored in 0.15% TritonX-100 in PBS (PBTr) at 4 °C. Tissues were permeated through incubation with 10 μg/ml Proteinase K at room temperature. Blocking was done with 4% BSA in PBTr for 2 h at room temperature. Specimens were immunostained with antibodies anti-phospho-Smad3 (ab52903, Abcam, Cambridge, UK), anti-GFP (A10262, Lifetechnology, CA) and anti-phospho-histone H3 (06-570, Millipore, MA), according to standard procedures. The following secondary antibodies were used: Goat Anti-Rabbit IgG, AP conjugate (Secondary Antibody Millipore™, 112448, Upstate™, MA), Alexa Fluor® 488 Goat Anti-Chicken IgG (H+L) Antibody (A1-1039, Lifetechnology, CA) and Polyclonal Swine Anti-Rabbit Immunoglobulins/TRITC (R0156, DakoCytomation, Glostrup, Denmark). Cell proliferation observed through IHC for pH3 and EdU assay was measured with Volocity 6.0 software and reported in supplemental tables and graphs. Statistical analyses were performed with GraphPad Prism software.

Results

Generation of a Smad3-dependent zebrafish reporter line

A Smad3-binding sequence, known to be regulated by TGFβ signaling, was identified in the regulatory region of human PAI-1

gene (Dennler et al., 1998). 12 repeats of this specific sequence, namely CAGA box, were cloned together with major late promoter Adenovirus (MLP) into a Gateway 5′ entry vector. These sequences were used to control the expression of fluorescent reporter genes, such as GFP and nls-mCherry. To prepare transgenic reporter lines Tg(*12xSBE:EGFP*)ia16 and Tg(*12xSBE:nlsmCherry*)ia15, a Tol2 vector containing TGFβ-responsive sequences was co-injected together with Tol2 Transposase mRNA into one-cell stage wild-type embryos. Mosaic transgenic fish were selected at roughly 24 h post-fertilization (hpf) and raised to the adult stage for screening. Positive founders were selected for the fluorescence level of their offspring in areas of known Smad3 activity (Fig. 1A) and by checking reporter expression to SB-431542, a known Alk4- and Alk5-inhibitor (Fig. 1B). It can be observed that at 15 hpf, GFP fluorescence is weak or undetectable but its mRNA staining is strong in the posterior trunk, while at 26 hpf fluorescence of GFP in the tail is stronger than its mRNA: this is because GFP expression follows its mRNA translation and is more stable. Founders for EGFP and nls-mCherry have been compared (Fig. S1 and Table 2), selected and used to follow *in vivo* Smad3-mediated TGFβ signaling. Notably, while a wide GFP expression is visible early after fertilization in the offspring of Tg(*12xSBE:EGFP*)ia16 females due to a maternal effect (Fig. S1), by mating heterozygous Tg(*12xSBE:EGFP*)ia16 males with a wild type females we obtain 50% of GFP+ embryos, without relevant differences in fluorescence among them (Fig. S1 and Table 3).

Pharmacological, genetic and molecular analyses show that Tg(12xSBE:EGFP)ia16 and Tg(12xSBE:nlsmCherry)ia15 are TGFβ/Smad3 reporters

We used different pharmacological and genetic approaches to demonstrate the specificity of Smad3-responsive transgenic lines.

Both Tg(*12xSBE:EGFP*)ia16 and Tg(*12xSBE:nlsmCherry*)ia15, also called 12xSBE lines, were tested at 24 hpf with an Alk4- and Alk5-inhibitor, SB-431542, and a more specific Alk5-inhibitor, LY364947 (not shown). After two days of treatment, the fluorescent reporter expression was drastically reduced compared to the control at the same stage of development (Fig. 1B). Moreover, RNA *in situ* hybridization shows a consistent reduction of reporter transcripts after 8 h of incubation with SB-431542 in Tg(*12xSBE:EGFP*)ia16 embryos treated at 24 hpf (Fig. 1C).

For genetic validation, the Tg(*12xSBE:EGFP*)ia16 line was crossed with *one-eyed-pinhead* (*oep*) and *chordin* (*dino*) mutant lines (Fig. S2). One-eyed-pinhead (TDGF1 or CFC1) is a cofactor of Nodal signaling, a subset of the TGFβ family, involved in mesendoderm specification, left–right axis specification and anterior-posterior axis orientation. In absence of zygotic *oep*, TGFβ-responsive line lacked GFP expression in cardiac mesoderm, underlying the role of *oep*-mediated TGFβ signaling in mesendoderm specification (Fig. S2B′′). On the other hand, the reporter expression was unchanged in the spinal cord (Fig. S2A′–B′), the formation of which does not require Nodal signaling (Jia et al., 2009).

Chordin is a major Bmp2/4 antagonist, expressed in zebrafish by shield stage. Both BMP and TGFβ1/2/3 belong to the TGFβ superfamily and have a similar transduction pathway. However, they require specific receptors and receptor-activated Smads. BMP and TGFβ have opposite roles in neural induction (negative and positive effects, respectively) (Schmidt et al., 2013). To evaluate the specificity of 12XSBE transgenic lines for TGFβ1/2/3-Smad2/3, reporter expression was evaluated in embryos missing the activity of *chordin*. Despite the obvious morphological changes due to axis specification disruption, we did not observe changes in fluorescence in the spinal cord of the mutants (Fig. S2A′–C′). Finally, treatments of 12XSBE embryos with LDN193189, an Alk2/3 inhibitor (Cuny et al., 2008), show no effect on the fluorescence of the reporter (Fig. S2D–E). This confirms the specificity of the reporter line for Smad3 rather than Smad1/5/8 and also confirms the idea of independent actions of TGFβ1/2/3 and BMP signaling on spinal cord development (Jia et al., 2009).

The 12xSBE lines were created using elements recognized by Smad3. To test their level of response and specificity, 1–2 cell-stage embryos were injected with morpholinos for *smad2/3a/3b/4* and their fluorescence was checked at 24 hpf (Fig. 2A and Table 3). The morpholinos for *smad2/3a/3b* have been already tested and previously validated and were able to induce different degrees of neural degeneration and growth retardation; morphant embryos fail to form floor plate, have eye malformations and bent notochord (Jia et al., 2008). A further validation for these morpholinos was performed through RT-PCR (MO-*smad2*) or immunohistochemistry (MO-*smad3a* and *3b*) (Fig. S3). When injected in the 12xSBE lines, MO-*smad2* had a partial effect on reporter activity in the neural tube, when given a high dose of morpholinos (Fig. 2 and Table 4). On the other hand, fluorescence was drastically reduced with MO-*smad3b* and completely abolished with MO-*smad3a*, demonstrating a strong specificity of the 12xSBE transgenic lines for Smad3 activity (Fig. 2A). Both zebrafish *smad3* isoforms, *3a* and *3b*, are expressed in the tail region (Pogoda and Meyer, 2002; Hsu et al., 2011) and the efficacy of MO-*smad3a* might be due to either a higher activity of the *smad3a* morpholino or to a higher expression/function of this gene. In all *smad3a*, *smad3b* and *smad2* morphants, no fluorescence was detected in the cardiac mesoderm. In fact these genes are known to play an important role in mesoderm specification and outflow tract formation (Jia et al., 2008; Zhou et al., 2011). To test if *smad2* can cooperate with *smad3* for the reporter expression, the lowest effective dosage of both morpholinos was coinjected in fertilized eggs of the Tg(*12xSBE:EGFP*)ia16 line. In *smad2/smad3a* coinjected embryos half the effect in the number of GFP positive embryos was obtained, when comparing the phenotype with embryos injected with a double dosage of MO-*smad3a* (Fig. S4 and Table S4). Furthermore, MO-*smad3a* injection at non teratogenic dose can abolish GFP expression, while in *smad2* morphants with a severe phenotype the reporter expression is only slightly affected (Fig. 2A). Thus, it can be assumed that Smad2 does not cooperate with Smad3a in 12XSBE reporter activation.

Smad4 is a common permissive factor for both TGFβ1/2/3 and BMP cascades, necessary for activation of all R-Smad-mediated signaling. Four different *smad4* morpholinos were designed and tested for their ability to abolish GFP expression in the TGFβ1/2/3-responsive line (not shown). MO3-*smad4*, specific for a splicing-donor site, was the most efficient and was used for knock down injections (Fig. 2A). This morpholino was tested through both RT-PCR (Fig. S3) and injection in BMP-responsive line (not shown). *smad4* morphants showed the most severe growth retardation, eye malformation and notochord defects when compared with *smad2/3a/3b*-morphants. The severe phenotype is possibly due to the pleiotropic permissive functions of Smad4.

To test the specificity of the Tg(*12xSBE:EGFP*)ia16 line for each TGFβ-associated transcription factor, *smad2*, *3a*, *3b* and *4* mRNAs were injected in fertilized eggs and GFP expression checked at 24 hpf under the epifluorescent microscope (Figs. S5 and S6). *smads* mRNAs injection resulted in different abnormalities in the embryos; *smad2* mRNA injections caused eye and head reductions, enlargement of yolk extension and caudal aedema; *smad3a* overexpression led to tail bending. *smad3b* mRNA injection seemed to be more deleterious than *smad3a*: the eyes and head are smaller and the notochord bent. Coinjection of *smad3a* and *3b* created a third phenotype with mixed defects: the anterior region normal, in the posterior a bent notochord and absence of yolk extension. GFP levels were unchanged by overexpressing *smad2*, *3a* and *4*. In contrast, injection of *smad3b* mRNA and, even more,

the coinjection of *smad3a* and *3b* mRNAs, increased GFP expression in tail and heart mesoderm and, notably, resulted in a strong ectopic expression of the reporter in the notochord of coinjected embryos (Figs. S5 and S6). Both normal (Fig. S5) and malformed (Fig. S6) embryos were used to draw these conclusions.

To demonstrate that reporter expression correlates with Smad3 activation at an intracellular level, expression of phosphorylated Smad3 was checked by immunohistochemistry (Fig. S7) at different stages (50% epiboly, tail bud, 13, 15, 24, 36 and 48 hpf) and compared to GFP expression in the same developmental stages of the Tg (*12xSBE:EGFP*)ia16 line. Although no fluorescence was observed earlier than 13 hpf, later stages show a correlated pattern of reporter/phospho-Smad3 expression in tail and heart mesoderm, spinal cord, eyes, hindbrain, cloaca and fin buds. It can be supposed that a certain level of Smad3 is required for reporter activation while lower levels are not sufficient to be detected with the Tg(*12xSBE:EGFP*)ia16 line. Furthermore, immunohistochemistry for phospho-Smad3 was performed in 24 hpf embryos and 48 hpf larvae of the Tg(*12xSBE:EGFP*)

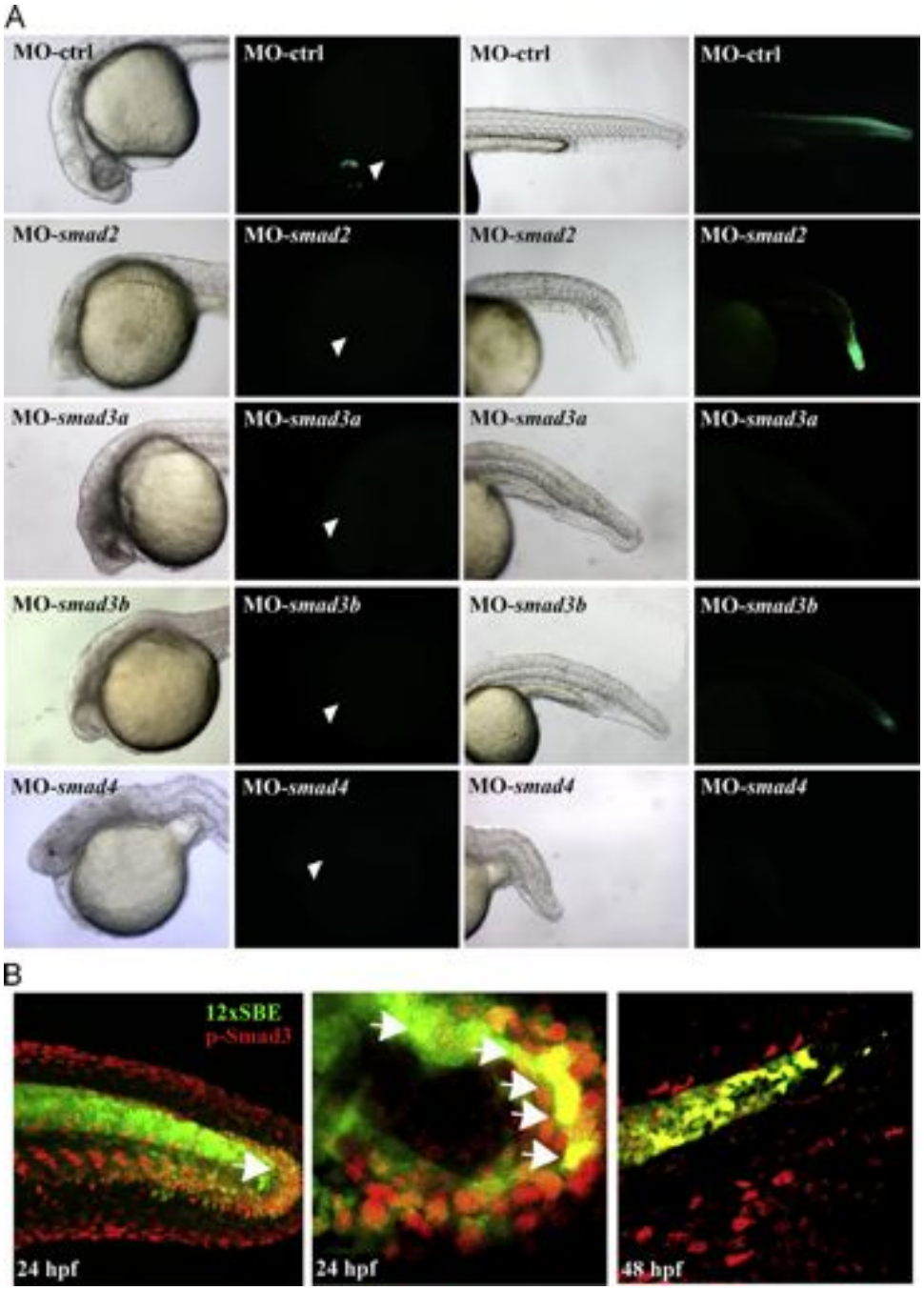

Fig. 2. Responsiveness of Tg(*12xSBE:EGFP*)ia16 line to Smad3. (A) Brightfield and fluorescent lateral images of *smad2*-, *smad3a*-, *smad3b*- and *smad4*-morphants at 24 hpf at the epifluorescent microscope, left to right. *smad2*, *3a* and *3b* morphants show a similar phenotype: anterior truncation, a curved shortened body axis, absence of floorplate and an enlarged intermediate cell mass. *smad4* morphants exhibit the most severe phenotype: similar characteristics of the other morphants accompanied with a shortened body due to BMP inhibition. Reporter expression is completely inhibited in *smad4* and *3a* morphants and strongly reduced in *smad3b* morphants. *smad2* morphants lack GFP expression in the cardiac mesoderm and telencephalon (white arrow head) and display a mild reduction in the neural tube. (B) Phosphorylated-Smad3 correlates to reporter expression in the 12xSBE line. Confocal lateral views of double fluorescent immunohistochemistry for GFP (green) and phosphorylated Smad3 (red) on embryo and larva tails at 24 and 48 hpf; zoomed views on the edge of the tail of a 24 hpf embryo. Arrowheads point to GFP/p-Smad3 double positive cells.

ia16 line (Fig. 2B): at both stages Smad3 activation was revealed in neural tube and tail mesoderm, with a decreasing rostro-caudal gradient, as seen in the transgenic lines. Reporter-expressing cells colocalized with phospho-Smad3 positive cells (Fig. 2B). In particular, at 24 hpf stage, it can be observed that coherently with the mechanistic sequence (Smad3 is phosphorylated, it enters the nucleus and activates transcription/translation of GFP), cells in which the phospho-Smad3 colocalizes with GFP are older than (rostral to) cells in which the phospho-Smad3 (in red) has just entered the nucleus, while they are younger than (caudal to) cells in which the phospho-Smad3 concentration has already decreased, leaving the reporter activated.

To further demonstrate the specificity of the 12xSBE lines, we induced the overexpression of either *smad7* or *smad3b* in 24 hpf embryos (Fig. 3). SMAD7 is an inhibitory SMAD able to block SMAD3-mediated TGFβ signaling by inhibiting phosphorylation of type I receptor, recruiting SMURF1 and 2 and leading to proteasomal degradation of ligand-receptor complexes (Yan et al., 2009). The Tg(*12xSBE:nlsmCherry*)ia15 line was crossed with a transgenic line expressing *smad7* and *YFP* coding sequences both under the control of the *hsp70* regulatory region. Heat-shocked larvae analyzed at the confocal microscope revealed a strong activation of YFP and a dramatic reduction of mCherry in the entire embryo (Fig. 3A–A″). Similarly, 1–2 cell stage embryos of the Tg(*12xSBE:nlsmCherry*)ia15 line were injected with a plasmid containing *smad3b* and *YFP* coding sequences under the control of the *hsp70* regulatory region and the resulting embryos heat shocked at the 24 hpf stage. As shown in Fig. 3, only heat-shocked embryos showed expression of the YFP. As a plasmid was injected the expression was mosaic. Notably, 12xSBE reporter expression levels were significantly increased in cells co-expressing YFP (*i.e.*, muscle in the trunk) meaning that *smad3* driven by the *hsp70* promoter causes cell-specific reporter activation (Fig. 3C–C″).

In conclusion, pharmacological, mutants, morpholinos and molecular analyses show that the zebrafish 12xSBE lines are *bona fide* TGFβ/Smad3 responsive, *in vivo*.

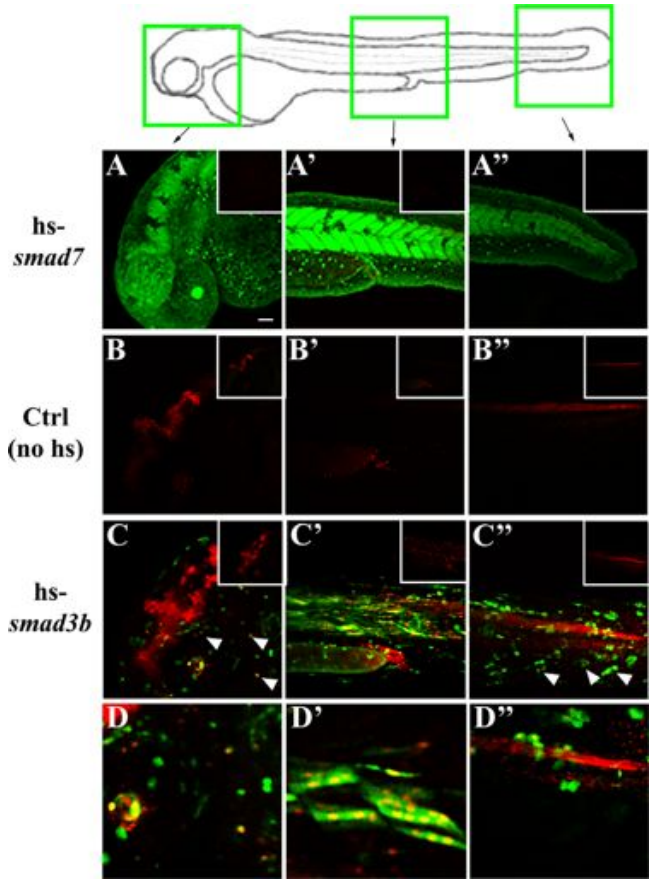

Fig. 3. Tg(*12xSBE:nls-mCherry*)ia15 line is responsive to *smad7* and *smad3b* overexpression. A–C″, confocal lateral views (Z-stacks) of 48 hpf double transgenic larvae, Tg(*12xSBE:nls-mCherry*)ia15/(*hs-Smad7/YFP*) or (*hs-Smad7/YFP*). As shown in the schematic 48 hpf larva, three areas have been analyzed: head, trunk and tail. Each picture shows the merge of YFP (green) and mCherry (red) and it is accompanied by a small figure (white square) representing mCherry fluorescence following the heat-shock. (A–A″) Confocal lateral views of 48 hpf double transgenic larvae, Tg(*12xSBE:nls-mCherry*)ia15/(*hs-Smad7/YFP*). Heat-shock causes a downregulation of the 12xSBE reporter (in red) and ubiquitous production of YFP (in green). (B–B″) Confocal lateral images of 48 hpf non-heat-shocked double transgenic larvae, Tg(*12xSBE:nls-mCherry*)ia15/(*hs-smad7/YFP*) and Tg(*12xSBE:nls-mCherry*)ia15/(*hs-smad3b/YFP*). Only non-heat-shocked Tg(*12xSBE:nls-mCherry*)ia15/(*hs-smad7/YFP*) is shown as a control. (C–C″) Confocal lateral views of 48 hpf heat-shocked double transgenic larvae, Tg(*12xSBE:nls-mCherry*)ia15/(*hs-smad3b/YFP*). The heat-shock leads to a *smad3b* overexpression confirmed by mosaic production of YFP. White arrow heads show ectopic expression in the head, trunk muscle and tail. (D–D″) Zoomed views (single planes) of Tg(*12xSBE:nls-mCherry*)ia15/(*hs-smad3b/YFP*) highlight the ectopic reporter expression induced by *smad3b* overexpression. Scale bar is 100 μm in A–C″; 20 μm in D–D″. Scale bar is 100 μm in A–B′, E–F′, G, H; 50 μm in C′–C″; and 20 μm in G′, H′.

During the first month of development Smad3-mediated TGFβ signaling is mainly observed in the nervous system

Then, we decided to analyze the spatio-temporal fluorescent activity of 12xSBE lines. While a wide GFP expression is visible early after fertilization in the offspring of Tg(*12xSBE:EGFP*)ia16 female carriers due to a maternal effect, a more specific fluorescence with zygotic origin appears at late somitogenesis (15 hpf) in the tail (both mesoderm and neural tube) and cardiac mesoderm region (Fig. 1A). At 26 hpf fluorescence is also visible in the telencephalic region. At 48 hpf reporter expression gradually extends to the entire neural tube, moving in a gradient that decreases from the tail (Fig. 1A). Tg(*12xSBE:EGFP*)ia16 and Tg(*12xSBE:nlsmCherry*)ia15 lines show a similar fluorescence expression pattern (Figs. 1 and S1). Differences can be seen in the exact time of expression in specific tissues due to the different accumulation/degradation dynamics of the two fluorescent proteins.

Outside of the central nervous system (CNS), fluorescence is distinguishable in the retina, lens and olfactory epithelium (Fig. S8D–E). Reporter-expressing cells are found in cardiac mesoderm at 24 hpf, where they give rise to the outflow tract (Zhou et al., 2011) (Fig. S8A–B′). In the heart region the reporter is still expressed at 3–4 dpf in the outflow tract and some cells distributed in the dorsal aorta (Fig. S8C–C′). Some fluorescent cells are also distinguishable in the jaws at 4 dpf (Fig. S8F–F′), while a weak GFP expression is visible in pectoral fins (Fig. S8G) and cloaca. Fins, cloaca and outflow tract are even more appreciable in Tg(*12xSBE:nlsmCherry*)ia15. In the tail and cardiac region, the reporter expression is also found in mesodermal cells. In fact, Smad3 signaling is known to be involved in mesoderm specification (Jia et al., 2008).

At about one month post-fertilization, fluorescence decreases in the entire central nervous system. It is still expressed at a low level in the ventral part of the CNS, particularly in the telencephalic region. At this stage, some muscle fibers of the median musculature start expressing the reporter gene (Fig. S8H). Indeed, the role of TGFb signaling in the control of muscle development is well-known (Ge et al., 2012; Hsu et al., 2011).

In adult fish, EGFP expression is localized at the edge of each vertebra and in the lens, while in Tg(*12xSBE:nlsmCherry*)ia15 fluorescence is detectable in the ventricular zone of the brain and telencephalic region (data not shown).

A more detailed observation of the Tg(*12xSBE:EGFP*)ia16 line with the confocal microscope gives a better understanding of brain

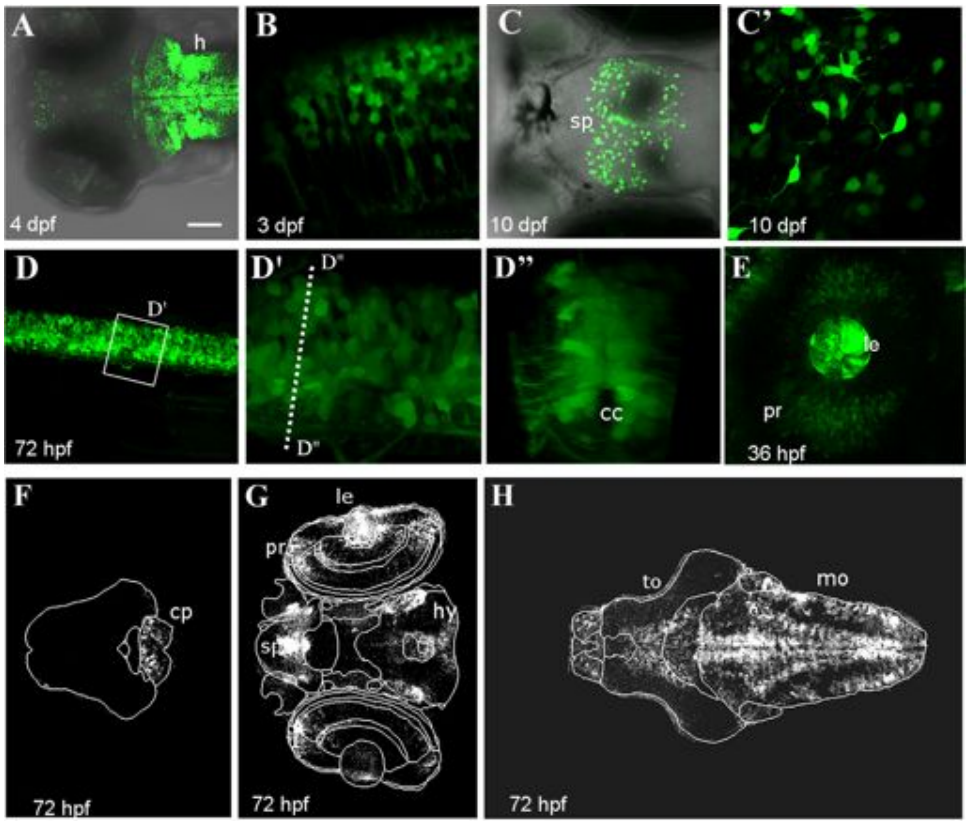

Fig. 4. Reporter expression during early larval development: central nervous system. Confocal images of brain and neural tube of Tg(*12xSBE:EGFP*)ia16 larvae at different stages of development. (A) Dorsal view of the brain of a 4 dpf larva (Z-stack). GFP is expressed in the hindbrain, diencephalon and telencephalon. (B) Zoomed lateral views of the hindbrain in a larva at 3 dpf (single plane). (C) Dorsal views of GFP-expressing cells in the subpallium of a 10 dpf larva (Z-stack). (C′) Zoomed dorsal view of GFP+ cells in the subpallium (Z-stack). (D) Lateral view of the neural tube in a 72 hpf larva (Z-stack). (D′–D″), 3D-reconstruction of the neural tube of D at the level of the dashed line (D′, lateral and, D″, sagittal view). Reporter expression is mainly localized around the central canal (cc). (E) Lateral view of an eye in a 36 hpf larva (Z-stack). (F–H) Single planes of Tg(12xSBE:EGFP)ia16 brain at 72 hpf. Images have been obtained with VibeZ software. h=hindbrain, sb=*subpallium*, cc=central canal, pr=proliferating retina, le=lens, hy=hypothalamus, to=*tectum opticum*, mo=*medulla oblongata*. Scale bar is 100 μm in A, D; 50 μm in C; 20 μm in E; and 10 μm in B, C′, D′–D″.

tissues activating Smad3 mediated TGFβ signaling. Anteriorly, the reporter is activated in the forebrain (*subpallium* and preoptic region) in the midbrain (*tegumentum* and *tectum opticum*), cerebellar plate, while in the hindbrain it is mainly expressed in the *medulla oblongata*, as seen in Fig. 4 and supplemental movie 1 obtained with the aid of Vibe-Z analyses (Ronneberger et al., 2012). In the neural tube, fluorescent cells occupy ventricular and transition zones, where neuronal precursors proliferate and neuroblasts start their differentiation, respectively (Fig. 4).

Supplementary material related to this article can be found online at http://dx.doi.org/10.1016/j.ydbio.2014.09.025.

Smad3 mediated TGFβ signaling is activated in neuronal precursors

Smad3 activation is known to have a neurotrophic effect on DOPAminergic neurons (Krieglstein et al., 2002; Tapia-Gonzalez et al., 2011), motor neurons (Ho et al., 2000) and interneurons (Garcia-Campmany and Marti, 2007) where it seems to be involved in axonal growth (motor neurons), differentiation process (interneurons) and positioning of differentiating neurons in the neural tube.

Thus, supported by the pattern expression of 12xSBE lines, we focused our attention to understanding the nature of cells in which the reporter is active. For this purpose, Tg(*12xSBE:nlsmCherry*)ia15 line was crossed with different transgenic lines expressing GFP under the control of promoters specific for neural populations, thus labeling different populations of progenitor, precursor and committed neural cells (*ngn1*, *neuroD*, *mnx1*). The reporter expression of each double transgenic was followed during the first week of development at the confocal microscope. The highest level of colocalization is seen with *neuroD* (Fig. S9) while no colocalization can be observed with *mnx1* (Fig. S9). On the other hand, *ngn1*, a marker labeling both small populations of progenitors and some differentiated neurons, reveals a significant degree of colocalization with the Smad3 reporter at the very tip of the tail, where neuronal progenitors develop (Fig. S9). To examine the dynamics of cells activating Smad3 mediated TGFβ signaling, we measured colocalization in the tail of 24 hpf double transgenic embryos. Our logic was thus: between 15 and 24 hpf stages, somites form at a constant rate. Therefore, the tail region was divided into pairs of somites and colocalization (expressed as Manders'coefficient referred to TGFβ on mCherry fluorescence) was evaluated in four regions starting from the edge of the tail toward the trunk (Fig. 5). The region of caudal somites is the earliest forming and the first activating Smad3 signaling in the neural tube. In our graphs, the colocalization in the region of the first pair of somites corresponds to the starting point of expression of TGFβ1/2/3 signaling (0 h) and has been plotted as a function of somite/time. As shown on the graphs (Fig. 5), at the time of its activation (time 0) TGFβ1/2/3 signaling has its highest colocalization with cells expressing *ngn1*, a marker typical of proliferating neural progenitors of the region (Korzh et al., 1998). By moving anteriorly, there is a progressive reduction of mCherry+/*ngn1*+ cells. Conversely, the number of mCherry+/*neuroD*+ cells increases when moving anteriorly (Fig. 5), and it is worth mentioning that *neuroD* is a good marker of all neuronal precursors (Korzh et al., 1998). In *mnx1*-expressing cells (differentiating motor neurons), mCherry expression remains very low in all four areas examined (Fig. 5). Notably, similar trends were observed when levels of colocalization of mCherry (TGFβ)

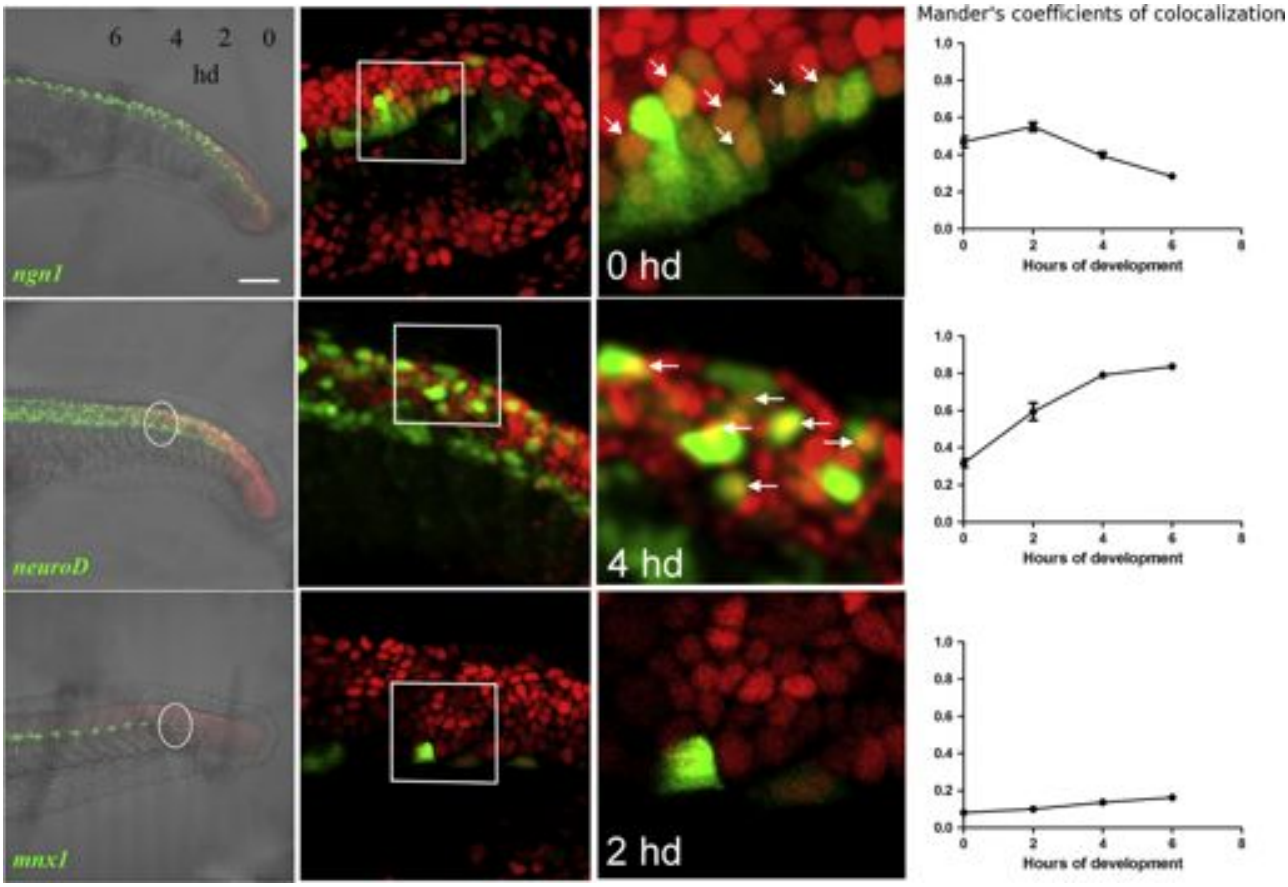

Fig. 5. Smad3 reporter is expressed in progenitors and precursors. Confocal lateral view of tail of double transgenic embryos obtained crossing Tg(*12xSBE:nls-mCherry*)ia15 to the following transgenics: Tg(*ngn1:GFP*)sb1, Tg(*−2.4 kb neurod:EGFP*) and Tg(*mnx1:GFP*)ml2. Colocalization was measured in the tail of 24 hpf double transgenic embryos with the following method. From 15 to 24 hpf, two somites are formed each hour. Tail region was divided in pairs of somites and colocalization (Manders'coefficient referred to TGFβ-mCherry fluorescence) evaluated in four of them (as white dotted circles) starting from the edge of the tail toward the trunk. For each time point, the average value of Manders' coefficient has been calculated from six double transgenic embryos and plotted on as a function of the corresponding hour of development (hd). Second column: magnification of specific regions (single plane). Third column: double fluorescent cells are shown with arrowheads (single plane). Developmental time of each magnification is indicated inside the panel. Fourth column: graphical representation of quantitative analysis as Mander's coefficients of the four developmental points; n=6 per each point. Scale bar is 100 μm in the first column, 20 μm in the second column, 10 μm in the last column.

and GFP (neuronal markers) at days 1, 2, 3 and 4 of development were compared (Fig. S9), confirming TGFβ is progressively turned on in the progenitor/precursor switch.

EdU assay shows that Smad3 mediated TGFβ signaling is a postmitotic signal

Once established that Smad3 mediated TGFβ signaling in the CNS is localized in committed neural precursors, we wanted to understand its role in development of neural cell lineage. Functional experiments with neuronal transgenic lines show that *smad3* activation is important for neurogenesis (Garcia-Campmany and Marti, 2007). To check whether *smad3* activation is involved in control of mitosis, we tested how the cell proliferation marker phospho-histone-3 (pH3) was affected in MO-*smad3a* injected embryos analyzed at 24 hpf or in larvae treated with LY364947 from 24 to 48 hpf. Results show that reporter signal (green) and pH3 immunofluorescence (red) do not colocalize (Figs. 6 and S4). Notably, blocking Alk4/5-Smad3 signaling leads to a significant increase of proliferating cells (Figs. 6 and S10). To further confirm this Smad3 mediated TGFβ effect, an EdU proliferation assay was performed on 20 hpf embryos treated with LY364947 at 12 hpf. Results show a strong increase of proliferation (Figs. 6 and S10). Thus, at early stages of development Alk4/5-Smad3 signaling seems to play an important role in regulating the cell cycle. We verified the function of Smad3 mediated TGFβ signaling on neural progenitor cell cycle by EdU proliferation assay on Tg(*12xSBE:EGFP*)ia16 embryos at 24 hpf (Fig. 6): embryos treated with EdU were fixed and stained after a chase of either 2 or 8 h. Cells stained after a chase of 2 h are roughly in S/G2 phase, while cells stained 8 h after the EdU pulse are in early G1 phase. Analysis of colocalization of GFP and EdU shows that proliferating cells (2 h in chase) do not express the reporter, while postmitotic cells (8 h in chase) do. In other words, at 24 hpf, the majority of cells with activated Smad3 are non proliferating but have just undergone mitosis, letting us conclude that Alk4/5-Smad3 in central nervous system development is mainly a postmitotic signal.

To confirm the hypothesis that Smad3 mediated TGFβ signaling blocks proliferation of some progenitor cells allowing their differentiation, *smad3a* morpholino was injected in 1–2 cell stage embryos of the transgenic lines Tg(*ngn1:GFP*)sb1, Tg(*−2.4 kb neurod:EGFP*) and Tg(*mnx1:GFP*)ml2 (Fig. 7). At 24 hpf *smad3a* morphant embryos show a decrease in GFP expression in motor neurons (*mnx1*), with defects in axon development and soma position in the neural tube (Fig. 7). The reduction of these cells in embryos treated with morpholino against *smad3a* is accompanied by a loss of their precursors as revealed by *neuroD* as well as an increase of neural progenitors revealed in the Tg(*ngn1:GFP*)sb1 line, particularly at the tail tip (Fig. 7 and Supplemental Table S5). The 12xSBE fish lines were also treated with Alk5-inhibitor LY364947 at 2 hpf and 24 hpf (Figs. 7 and S11). As shown in the figure, the results of these chemical treatments agree with those of the *smad3a* morpholino: an increase of *ngn1*+ at the tail end together with a concomitant decrease of *neuroD*+ and *mnx1*+ cells. In conclusion, both approaches gave

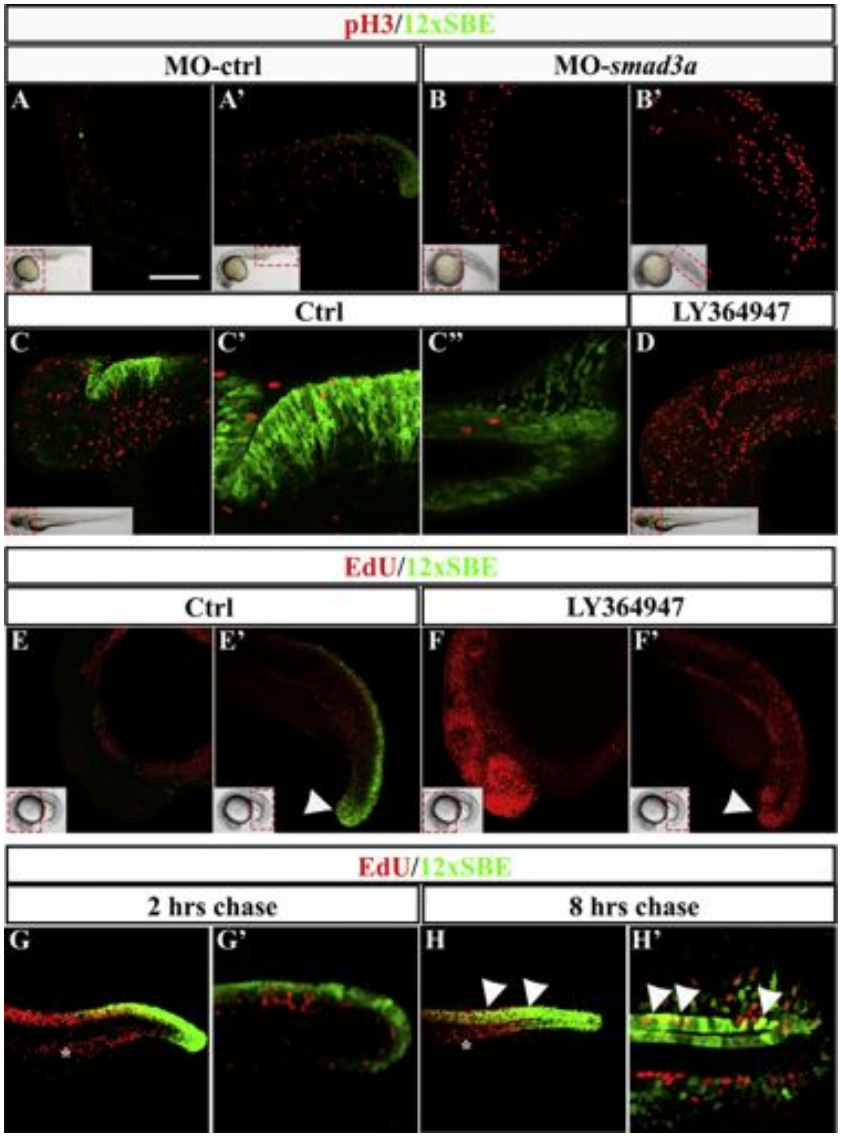

Fig. 6. Smad3/TGFβ signaling is mainly active in post-mitotic cells. (A–B′) Confocal lateral views of immunofluorescence for GFP (green) and phospho-Histone3 (pH3, red) on Tg(*12xSBE:EGFP*)ia16 embryos injected at 1–2 cell stage either with the control (A), or *smad3a*-morpholino (B). For each confocal picture (Z-stack), a small brightfield view of a morphant embryo shows which area is displayed (red dashed line). (C–D) Confocal lateral views of immunofluorescence for GFP (green) and pH3 (red) on 2 dpf larva of Tg (*12xSBE:EGFP*)ia16 line treated with either DMSO (C) or LY364947 (D) at 24hpf. For each confocal picture (Z-stack), a small brightfield view of a 48 hpf larva shows which area is displayed (red dashed line). (C′ and C″) Confocal zoomed views (single plane) of hindbrain and tail, respectively, of immunofluorescence for GFP (green) and pH3 (red) on DMSO-treated larva of the 12xSBE line. (E–F) Confocal lateral views of the head (E, F) or tail (E′, F′) regions after EdU labeling on 20 hpf embryos treated at 12 hpf either with DMSO (E, E′) or LY364947 (F, F′). For each confocal picture (Z-stack), a small brightfield view of a morphant embryo shows which area is displayed (red dashed line). (G, H) confocal lateral images (Z-stack) of pulse and chase EdU assay on 24 hpf embryos of Tg(*12xSBE:EGFP*)ia16 line. Embryos have been fixed after a chase of either 2 (G–G′) or 8 (H–H′) hours (hrs) and immunostained for EdU (red) and GFP (green). EdU+ cells fixed after 2 h are roughly in S/G2 phase, while EdU+ cells fixed after 8 h of chase are post-mitotic. (G′, H′) Zoomed view (single plane) of Tg(*12xSBE:EGFP*)ia16 tail after 2 or 8 h chase. Scale bar is 100 μm in A–B′, E–F′, G, H; 50 μm in C′–C″; 20 μm in G′, H′. Quantification is presented in Supplemental Table S4.

similar results on the role of Alk4/5-Smad3 mediated TGFβ signaling in controlling the progenitor/precursor switch.

Discussion

Through this work we have developed zebrafish transgenic line 12xSBE, responsive to Smad3 mediated TGFβ1/2/3-Alk4/5 signaling. Through pharmacological, genetic and molecular characterization we have seen that this transgenic line reports Smad3 activity and can be used to follow the TGFβ1/2/3 branch of signaling *in vivo*, at single cell resolution.

Treatment with chemical Alk4- and Alk5-inhibitors (SB-431542 and LY-364947), which blocks phosphorylation of Smad3 by TGFβ1/2/3 type-I receptors, inhibits reporter expression: the transcription of the reporter gene is abolished within 8 h of treatment with SB-431542 (Fig. 1C), while fluorescence level is reduced after 1 day of treatment (data not shown) and completely blocked after 2 days (Fig. 1B). Conversely, treatments with LDN193189 (a specific Alk2,3 inhibitor) left the fluorescence unchanged (Fig. S2). Moreover, immunohistochemistry for phospho-Smad3 has demonstrated that this transcription factor is present during gastrulation, though the quantity is insufficient to activate reporter transcription and translation of the Tg(*12xSBE:EGFP*)ia16 line at detectable fluorescence levels (Fig. S7). At the tail bud neither phospho-Smad3 nor reporter expressions are appreciable (Fig. S7). At 13 hpf phospho-Smad3 and GFP are both expressed in the mesoderm (cardiac and tail) and spinal cord (Fig. S7). At the same stage, while phospho-Smad3 is clearly

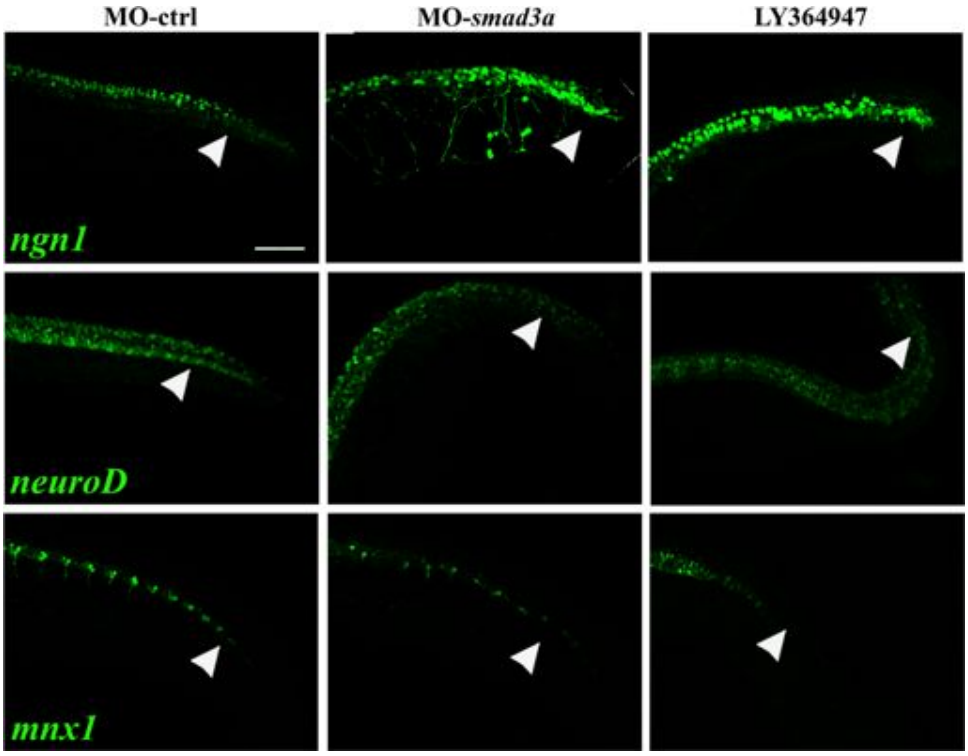

Fig. 7. *In vivo* blocking of Smad3/TGFβ signaling impairs neuronal differentiation during early embryonic development. Confocal Z-stack tail images of 24 hpf transgenic embryos expressing GFP under control of neuronal promoter: *ngn1*, *neuroD*, and *mnx1*. Embryos were injected with morpholinos for *smad3a* at 1–2 cell stage or treated at 2 hpf with Alk5-inhibitor LY364947. As shown with an arrowhead, morpholinos and drug treatment give similar results: increase of proliferative cells (*ngn1*) at tail tip, decrease of differentiating cells (*neuroD*) and reduction of late differentiating motor neurons (*mnx1*). *ngn1* is Tg(*ngn1:GFP*)sb1. *neuroD* is Tg(*−2.4 kb neurod:EGFP*). *mnx1* is Tg (hlxb9:GFP)ml2. Quantification of each frame is shown in Supplemental Table S3. Scale bar is 100 μm in all the images.

visible in the eye, the reporter is not. This difference could be explained in many ways: an immunohistochemistry artefact or phospho-Smad3 levels are not sufficient to induce reporter expression. It is possible Smad4 is missing or a phospho-Smad3 corepressor is inhibiting transcription; in fact the lens and retina start to be GFP positive from 24–26 hpf. Similar restrictions could explain the presence of phospho-Smad3+cells in the entire tail mesoderm, while the reporter is limited to the tail edge. The specificity of the reporter is also confirmed by *smads* mRNA injection in the Tg(*12xSBE:EGFP*)ia16 line (Figs. S5 and S6). *smad3b* mRNA and *smad3a* and *3b* mRNAs together can ectopically activate the reporter. Notably, this can happen only if embryos are injected with Smad3 mRNA, while Smad4 and 2 have no effect in reporter activation. Through fluorescent immunohistochemistry we have demonstrated reporter expression follows the nuclear localization of phospho-Smad3 (Fig. 2B). The partial colocalization of GFP and phospho-Smad3 is expected, as it takes time for phospho-Smad3 expression to overcome both a threshold level of the transcription factor and the time to have an appreciable transcription and translation of the reporter.

Genetic and molecular approaches gave us more details about reporter expression in the transgenic line. GFP expression of Tg (*12xSBE:EGFP*)ia16 line has been tested in two different genetic backgrounds: *one-eyed-pinhead* (*oep*) and *chordin* (*dino*) mutants. One-eyed-pinhead (Oep) is an EGF-CFC protein and cofactor necessary for Nodal/Activin branch of TGFβ signaling, a cascade culminating with the activation of Smad2 rather than Smad3 (Fei et al., 2010). In *oep* mutants of the transgenic line, GFP expression was absent in the cardiac mesoderm (Fig. S2); no significant changes in expression levels were observed in the neural tube, where Smad3 activity seems to be independent from Nodal ligands. Although it was demonstrated that Nodal signaling is involved in anterior neural tube closure, neuroectoderm specification (Aquilina-Beck et al., 2007) and hypothalamus development (Rohr et al., 2001), it acts mainly through Smad2 (Fei et al., 2010) and seems dispensable to spinal cord induction (Jia et al., 2009).

As BMP and TGFβ1/2/3 show a similar transduction pathway but different types of receptors, R-Smads and their relative target sequence in the genome, we tested the effects of BMP activation on Smad3-mediated reporter expression by analyzing mutants of *chordin*, a BMP2/4 antagonist. It was demonstrated that Smad2/3 upregulate BMP inhibitors, such as *chordin*, BMP inhibition is important for neural induction (Jia et al., 2009; Cruz et al., 2010) and levels of GFP expression in the neural tube of *dino* mutants compare with that of sibs, confirming the specificity of 12xSBE transgenic line for TGFβ1/2/3-associated R-Smads (Fig. S2).

Morpholino-mediated knock-down of R-Smads and Co-Smad confirmed the specificity of both Tg(*12xSBE:EGFP*)ia16 and Tg(*12xSBE:nlsmCherry*)ia15 lines for Smad3/4. Concerning R-Smads morphants, the transgenic lines seemed to be sensitive to both zebrafish isoforms of *smad3*: *smad3a* and *smad3b*. When embryos were injected with *smad3a* morpholino, they failed to express both EGFP and mCherry (Fig. 2A and not shown). Knock-down of *smad3b* strongly inhibited reporter expression, which was limited to the tip of the tail. We envisage two possible explanations for these results: (1) a higher efficacy of the *smad3a* morpholino with respect to the *smad3b* one; (2) different levels of genetic additivity for the two loci allow *smad3a* to partially compensate for *smad3b* absence in the spinal cord, but not *viceversa*.

Though the transgenic lines were designed with Smad3-responsive sequence (Dennler et al., 1998), the injection of *smad2* morpholino inhibited reporter expression in the cardiac mesoderm and interfered with fluorescence in the tail region (Figs. 2A and S3). In contrast to what is seen for SMAD2 and 3 in the chicken neural tube (Lan, 2011) (Miguez et al., 2013), only high doses of

smad2 morpholino give an appreciable reduction of 12xSBE-depending reporter expression (Table 4). However, the different techniques used to inhibit and study Smad2 in zebrafish (this work) and chicken (Miguez et al., 2013) (*i.e.,* morpholino *vs.* short-hairpin RNA; microinjection of eggs *vs.* electroporation of neural tube; stable line *vs.* transient expression) can explain the differences. Alternatively, Smad2-3a-3b and 4 interact in different ways in neural tube formation of the two animals.

Coinjection of the lowest effective doses of *smad2* and *3a* morpholinos showed that the reporter is strictly *smad3/4* dependant with no *smad2* dependent reporter activity. *smad2* morpholino induces a reporter decrease only when it causes a severe phenotype. On the other hand, *smad3a* morpholino can inhibit reporter expression at non teratogenic doses. Moreover, overexpression of *smad2* and *4* by injection of the corresponding mRNAs did not alter GFP expression. Smad4 is indeed permissive for the Smad3 dependant GFP expression. Interestingly, only *smad3b* overexpression causes a reporter increase, while *smad3a* can induce GFP production only in combination with *smad3b*. As seen in morpholino-directed knockdown, the two *smad3* isoforms seem to have similar, but not identical roles in the activation of the reporter expression.

In any case, the 12xSBE line will be a useful tool, together with a still missing Smad2 reporter line (possibly based on activin response elements, ARE) (Chen et al., 1996), to dissect the functional interactions between the TGFβ family specific transcriptional effectors *in vivo*.

Characterization of Tg(*12xSBE:nlsmCherry*)ia15 line has been completed by overexpressing *smad7* and *smad3b*. Overexpression of *smad7* caused a drastic reduction of reporter activity in all domains (Fig. 3). On the other hand, overexpression of *smad3b* by plasmid injection led to a mosaic activity of *smad3b* and, consequently, of the reporter (Fig. 3). An ectopic expression of mCherry in Smad3-competent cells, as was evident, supports the idea that muscle cells do not possess epigenetic mechanisms to inactivate this pathway.

Confocal observations of the transgenic line show that in the neural tube the reporter is active in cells surrounding the ventricular zone (Fig. 4). This area is known to be a region in which genetic signals lead neural progenitor cells to exit the cell cycle and begin differentiation (Schmidt et al., 2013). To understand the role of Smad3 activation in this area, the Tg(*12xSBE:nlsmCherry*)ia15 line has been crossed with different transgenic lines expressing GFP in different neuronal cells: Tg(*ngn1:GFP*)sb1, Tg(*−2.4 kb neurod:EGFP*) and Tg(*mnx1:GFP*)ml2. The observation of patterns of colocalization has shown that reporter expression was activated in differentiating neurons (*neuroD+* cells) (Fig. S9). Colocalization of Smad3-responsive cells with *neuroD+* cells was high while a significant degree of colocalization was measured with *ngn1+* cells at the tip of the tail, where neuronal progenitors arise (Fig. S9). On the other hand, committed cells (*mnx1+*) seem to be Smad3/TGFβ1/2/3 negative (Fig. S9). From these observations we suspected that TGFβ1/2/3 signaling could be active in *ex*-progenitor cells, which exit the cell cycle and start differentiating. This hypothesis was confirmed after analyzing Smad3 signaling in the tail of double transgenic embryos at 24 hpf, using somites as a molecular clock (Fig. 5). At the onset of Smad3 signaling ($t=0$), progenitor cells (*ngn1+*) coexpressed the reporter signal (Fig. 5). Colocalization was maintained with differentiating neuronal cells (*neuroD+*) (Fig. 5). Committed motor neurons (*mnx1+*) on the other hand, did not show significant colocalization at any of the time-points examined (Fig. 5).

The Smad3 control of proliferation is crucial during early-postnatal differentiation of cerebellar neurons into postmitotic neurons, by activation of cyclin-dependent kinase inhibitors p21, p27 and markers of neuronal differentiation (Ueberham and Arendt, 2013). A clear inhibitory function of Smad3 on neural progenitors proliferation was observed in chickens developing a spinal cord, where Smad3 also promotes differentiation of selected neurons and glia (Garcia-Campmany and Marti, 2007). Both immunohistochemistry for phospho-hystone3 on *smad3a* morphant embryos at 24 hpf (Fig. 7A–B′) and LY364947-treated larvae at 48 hpf (Fig. 7C–D′) and EdU proliferation assay on embryos treated with Alk5 inhibitor, LY364947, (Fig. 7E–F′) showed a massive increase of proliferating cells in many tissue compartments, the nervous system (NS) included. All these experiments have confirmed that Alk4/5-Smad3 signaling negatively regulates the cell cycle and is inactive in proliferating cells. Colocalization studies have indicated that Smad3-responsive cells mainly correspond to differentiating cells rather than proliferating and mature cells in the NS. Pulse and chase EdU proliferation assay has confirmed that in 24 hpf Tg(*12xSBE:EGFP*)ia16 embryos GFP-expressing cells are post-mitotic for the most part (Fig. 7G–H′). We can conclude that Smad3 acts on the cell cycle by controlling cell proliferation and it is expressed postmitotically at 24 hpf.

Having demonstrated that Smad3 is activated in the NS by differentiating cells, we have carried out some functional *in vivo* studies blocking Alk4/5-Smad3 activity in embryos of the transgenic lines used for colocalization measurements: Tg(*ngn1:GFP*)sb1, Tg(*−2.4 kb neurod:EGFP*) and Tg(*mnx1:GFP*)ml2. Both genetic and pharmacological TGFβ1/2/3 inhibition led us to similar conclusions (Fig. 7): Smad3 mediated TGFβ signaling is important to maintain a balance between progenitor and committed cells and a decrease in TGFβ signaling activity increases the number of undifferentiated cells (*ngn1+* cells) and a decrease of committed cells (*mnx1+*).

Another conclusion from our studies is about Smad3a and 3b roles in NS development: both Smad3 isoforms can recognize CAGA box and direct reporter expression in the neural tube. Functional *in vivo* experiments with transgenics confirmed that the two isoforms are equally involved in neurogenesis as the effects on the neural markers expression seemed to be very similar. Coinjection of the 2 morpholinos did not cause a further impairment in the neural tube formation, while the embryo body appeared to be more severely altered (shortened embryo, smaller malformed head) (not shown). This let us conclude that at least in neural tube formation Smad3a and 3b have similar levels of additive genetic effects.

Through these assays, we can hypothesize that the 12xSBE line is responsive to TGFβ1/2/3-Alk4/5-Smad3- signaling drugs, depends on Smad3 activation and it is inhibited by Smad7. In addition, both zebrafish Smad3 isoforms seem to recognize CAGA box with similar efficacy and participate equally in differentiation of the neural tube. According to this data, Smad3 mediated TGFβ signaling seems to have a role in CNS development by controlling the progenitor to precursor switch.

Finally, this work aims to showcase an alternative approach in studying biological mechanisms. The current paradigm of dissecting gene function usually begins with gene identification, the definition of its expression domain, followed by knockdown and description of the phenotypic effects. However, this approach is limited if one considers that dissection of gene functions and phenotypes needs the precise identification of the cells in which the genes or pathways are operating, as well as the understanding of the temporal dynamic of gene activity computed by cells *in vivo*. The approach used in this work is an attempt to overcome this limitation: we started from the strongest expression of a functional reporter to identify the tissues in which a transcription factor (Smad3) is activated by a main developmental signaling pathway (TGFβ). Here we analyzed the functions of Smad3 in previously neglected tissues and cell types – the periventricular cells of the neural tube -that we reveal as main targets of TGFβ ligands, thus unveiling targets of pleiotropic signals coming from a different tissues equipped with multiple inducing abilities.

Acknowledgments

We would like to thank Stefano Piccolo and his group for the great help in discussion, as well as Dott. Luigi Pivotti, Dott. Martina Milanetto and Emily Bowe for their precious support in this work. We are grateful to Wolfgang Driever for the access to the Vibe-Z platform.

The work is granted by the European Union Project ZF-HEALTH CT-2010-242048, by the Cariparo Project "An *in vivo* reporter platform for cancer studies and drugs screening" and by the AIRC Project IG 10274.

Appendix A. Supporting information

Supplementary data associated with this article can be found in the online version at http://dx.doi.org/10.1016/j.ydbio.2014.09.025.

References

Aquilina-Beck, A., Ilagan, K., Liu, Q., Liang, J.O., 2007. Nodal signaling is required for closure of the anterior neural tube in zebrafish. BMC Dev. Biol. 7, 126.
Chen, Y., Lebrun, J.J., Vale, W., 1996. Regulation of transforming growth factor beta- and activin-induced transcription by mammalian Mad proteins. Proc. Natl. Acad. Sci. USA 93, 12992–12997.
Cruz, C., Maegawa, S., Weinberg, E.S., Wilson, S.W., Dawid, I.B., Kudoh, T., 2010. Induction and patterning of trunk and tail neural ectoderm by the homeobox gene eve1 in zebrafish embryos. Proc. Natl. Acad. Sci. USA 107, 3564–3569.
Cuny, G.D., Yu, P.B., Laha, J.K., Xing, X., Liu, J.F., Lai, C.S., Deng, D.Y., Sachidanandan, C., Bloch, K.D., Peterson, R.T., 2008. Structure–activity relationship study of bone morphogenetic protein (BMP) signaling inhibitors. Bioorg. Med. Chem. Lett. 18, 4388–4392.
Dennler, S., Itoh, S., Vivien, D., ten Dijke, P., Huet, S., Gauthier, J.M., 1998. Direct binding of Smad3 and Smad4 to critical TGF beta-inducible elements in the promoter of human plasminogen activator inhibitor-type 1 gene. EMBO J. 17, 3091–3100.
Dick, A., Mayr, T., Bauer, H., Meier, A., Hammerschmidt, M., 2000. Cloning and characterization of zebrafish smad2, smad3 and smad4. Gene 246, 69–80.
Dunn, N.R., Koonce, C.H., Anderson, D.C., Islam, A., Bikoff, E.K., et al., 2005. Mice exclusively expressing the short isoform of Smad2 develop normally and are viable and fertile. Genes Dev. 19, 152–163.
Dunn, K.W., Kamocka, M.M., McDonald, J.H., 2011. A practical guide to evaluating colocalization in biological microscopy. Am. J. Physiol. Cell Physiol. 300, C723–C742.
Fei, T., Zhu, S., Xia, K., Zhang, J., Li, Z., Han, J.D., Chen, Y.G., 2010. Smad2 mediates Activin/Nodal signaling in mesendoderm differentiation of mouse embryonic stem cells. Cell Res. 20, 1306–1318.
Fleisch, M.C., Maxwell, C.A., Barcellos-Hoff, M.H., 2006. The pleiotropic roles of transforming growth factor beta in homeostasis and carcinogenesis of endocrine organs. Endocr. Relat. Cancer 13, 379–400.
Garcia-Campmany, L., Marti, E., 2007. The TGFbeta intracellular effector Smad3 regulates neuronal differentiation and cell fate specification in the developing spinal cord. Development 134, 65–75.
Ge, X., Vajjala, A., McFarlane, C., Wahli, W., Sharma, M., Kambadur, R., 2012. Lack of Smad3 signaling leads to impaired skeletal muscle regeneration. Am. J. Physiol. Endocrinol. Metab. 303, E90–E102.
Gomes, F.C., Sousa Vde, O., Romao, L., 2005. Emerging roles for TGF-beta1 in nervous system development. Int. J. Dev. Neurosci. 23, 413–424.
Herman, J.M., Fan, K.Y., Wild, A.T., Wood, L.D., Blackford, A.L., Donehower, R.C., Hidalgo, M., Schulick, R.D., Edil, B.H., Choti, M.A., et al., 2013. Correlation of Smad4 status with outcomes in patients receiving erlotinib combined with adjuvant chemoradiation and chemotherapy after resection for pancreatic adenocarcinoma. Int. J. Radiat. Oncol. Biol. Phys. 87, 458–459.
Hinck, A.P., 2012. Structural studies of the TGF-betas and their receptors – insights into evolution of the TGF-beta superfamily. FEBS Lett. 586, 1860–1870.
Ho, T.W., Bristol, L.A., Coccia, C., Li, Y., Milbrandt, J., Johnson, E., Jin, L., Bar-Peled, O., Griffin, J.W., Rothstein, J.D., 2000. TGFbeta trophic factors differentially modulate motor axon outgrowth and protection from excitotoxicity. Exp. Neurol. 161, 664–675.
Hsu, R.J., Lin, C.C., Su, Y.F., Tsai, H.J., 2011. dickkopf-3-related gene regulates the expression of zebrafish myf5 gene through phosphorylated p38a-dependent Smad4 activity. J. Biol. Chem. 286, 6855–6864.
Jia, S., Ren, Z., Li, X., Zheng, Y., Meng, A., 2008. smad2 and smad3 are required for mesendoderm induction by transforming growth factor-beta/nodal signals in zebrafish. J. Biol. Chem. 283, 2418–2426.
Jia, S., Wu, D., Xing, C., Meng, A., 2009. Smad2/3 activities are required for induction and patterning of the neuroectoderm in zebrafish. Dev. Biol. 333, 273–284.
Katsuno, M., Adachi, H., Banno, H., Suzuki, K., Tanaka, F., Sobue, G., 2011. Transforming growth factor-beta signaling in motor neuron diseases. Curr. Mol. Med. 11, 48–56.
Kimmel, C.B., Ballard, W.W., Kimmel, S.R., Ullmann, B., Schilling, T.F., 1995. Stages of embryonic development of the zebrafish. Dev. Dyn. 203, 253–310.
Korzh, V., Sleptsova, I., Liao, J., He, J., Gong, Z., 1998. Expression of zebrafish bHLH genes ngn1 and nrd defines distinct stages of neural differentiation. Dev. Dyn. 213, 92–104.
Krieglstein, K., Strelau, J., Schober, A., Sullivan, A., Unsicker, K., 2002. TGF-beta and the regulation of neuron survival and death. J. Physiol. 96, 25–30.
Kwan, K.M., Fujimoto, E., Grabher, C., Mangum, B.D., Hardy, M.E., Campbell, D.S., Parant, J.M., Yost, H.J., Kanki, J.P., Chien, C.B., 2007. The Tol2kit: a multisite gateway-based construction kit for Tol2 transposon transgenesis constructs. Dev. Dyn. 236, 3088–3099.
Lan, H.Y., 2011. Diverse roles of TGF-beta/Smads in renal fibrosis and inflammation. Int. J. Biol. Sci. 7, 1056–1067.
Lee, K.L., Lim, S.K., Orlov, Y.L., Yit le, Y., Yang, H., Ang, L.T., Poellinger, L., Lim, B., 2011. Graded Nodal/Activin signaling titrates conversion of quantitative phospho-Smad2 levels into qualitative embryonic stem cell fate decisions. PLoS Genet. 7, e1002130.
Liu, X., Sun, Y., Constantinescu, S.N., Karam, E., Weinberg, R.A., Lodish, H.F., 1997. Transforming growth factor beta-induced phosphorylation of Smad3 is required for growth inhibition and transcriptional induction in epithelial cells. Proc. Natl. Acad. Sci. USA 94, 10669–10674.
Manders, E.M.M., Verbeek, F.J., Aten, J.A., 1993. Measurement of co-localization of objects in dual-colour confocal images. J. Microsc. 169, 375–382.
Miguez, D.G., Gil-Guinon, E., Pons, S., Marti, E., 2013. Smad2 and Smad3 cooperate and antagonize simultaneously in vertebrate neurogenesis. J. Cell Sci. 126, 5335–5343.
Moustakas, A., Heldin, C.H., 2009. The regulation of TGFbeta signal transduction. Development 136, 3699–3714.
Nomura, M., Li, E., 1998. Smad2 role in mesoderm formation, left-right patterning and craniofacial development. Nature 393, 786–790.
Pogoda, H.M., Meyer, D., 2002. Zebrafish Smad7 is regulated by Smad3 and BMP signals. Dev. Dyn. 224, 334–349.
Rohr, K.B., Barth, K.A., Varga, Z.M, Wilson, S.W., 2001. The nodal pathway acts upstream of hedgehog signaling to specify ventral telencephalic identity. Neuron 29, 341–351.
Ronneberger, O., Liu, K., Rath, M., Ruebeta, D., Mueller, T., Skibbe, H., Drayer, B., Schmidt, T., Filippi, A., Nitschke, R., et al., 2012. ViBE-Z: a framework for 3D virtual colocalization analysis in zebrafish larval brains. Nat. Methods 9, 735–742.
Schier, A.F., Neuhauss, S.C., Harvey, M., Malicki, J., Solnica-Krezel, L., Stainier, D.Y., Zwartkruis, F., Abdelilah, S., Stemple, D.L., Rangini, Z., et al., 1996. Mutations affecting the development of the embryonic zebrafish brain. Development 123, 165–178.
Schmidt, R., Strahle, U., Scholpp, S., 2013. Neurogenesis in zebrafish – from embryo to adult. Neural Dev. 8, 3.
Schulte-Merker, S., Lee, K.J., McMahon, A.P., Hammerschmidt, M., 1997. The zebrafish organizer requires chordino. Nature 387, 862–863.
Song, J., 2007. EMT or apoptosis: a decision for TGF-beta. Cell Res. 17, 289–290.
Tapia-Gonzalez, S., Giraldez-Perez, R.M., Cuartero, M.I., Casarejos, M.J., Mena, M.A., Wang, X.F., Sanchez-Capelo, A., 2011. Dopamine and alpha-synuclein dysfunction in Smad3 null mice. Mol. Neurodegener. 6, 72.
ten Dijke, P., Hill, C.S., 2004. New insights into TGF-beta-Smad signaling. Trends Biochem. Sci. 29, 265–273.
Thisse, C., Thisse, B., Schilling, T.F., Postlethwait, J.H., 1993. Structure of the zebrafish snail1 gene and its expression in wild-type, spadetail and no tail mutant embryos. Development 119, 1203–1215.
Town, T., Laouar, Y., Pittenger, C., Mori, T., Szekely, C.A., Tan, J., Duman, R.S., Flavell, R.A., 2008. Blocking TGF-beta-Smad2/3 innate immune signaling mitigates Alzheimer-like pathology. Nat. Med. 14, 681–687.
Ueberham, U., Arendt, T., 2013. The role of Smad proteins for development, differentiation and dedifferentiation of neurons. In: Wislet-Gendebien, Dr Sabine (Ed.), Trends in Cell Signaling Pathways in Neuronal Fate Decision. InTech, Rijeka, Croatia (EU), ISBN: 978-953-51-1059-0, http://dx.doi.org/10.5772/54532.
Watabe, T., Miyazono, K., 2009. Roles of TGF-beta family signaling in stem cell renewal and differentiation. Cell Res. 19, 103–115.
Yan, X., Liu, Z., Chen, Y., 2009. Regulation of TGF-beta signaling by Smad7. Acta Biochim. Biophys. Sin. 41, 263–272.
Zhu, Y., Richardson, J.A., Parada, L.F., Graff, J.M., 1998. Smad3 mutant mice develop metastatic colorectal cancer. Cell 94, 703–714.
Zhou, Y., Cashman, T.J., Nevis, K.R., Obregon, P., Carney, S.A., Liu, Y., Gu, A., Mosimann, C., Sondalle, S., Peterson, R.E., et al., 2011. Latent TGF-beta binding protein 3 identifies a second heart field in zebrafish. Nature 474, 645–648.